Repeated eye reduction events reveal multiple pathways to degeneration in a family of marine snails

Lauren Sumner-Rooney[1,2]*, Julia D. Sigwart[1,2], Jenny McAfee[2], Lisa Smith[3] and Suzanne T. Williams[4]

[1]School of Biological Sciences, Queen's University Belfast, Belfast, BT9 7BL, Northern Ireland.

[2]Queen's University Marine Laboratory, Queen's University Belfast, Portaferry, Co. Down, BT22 1PF, Northern Ireland.

[3]Core Research Facility, Natural History Museum, Cromwell Road, London, SW7 5BD, UK.

[4]Department of Life Sciences, Natural History Museum, Cromwell Road, London, SW7 5BD, UK

*Corresponding author. Email: lsumnerrooney01@qub.ac.uk

Running title: Eye reduction in a family of marine snails

Keywords: Eye loss, eye evolution, deep sea, Vetigastropoda, Solariellidae

Word count: 9650 (5425 excl. tables, references, figure legends)

Figures: 5

Tables: 1

Sequence data are stored on Genbank (accession numbers included in Table 1 and SD6).

Supplementary data files will be stored on Dryad.

Abstract

Eye reduction occurs in many troglobitic, fossorial and deep-sea animals but there is no clear consensus on its evolutionary mechanism. Given the highly conserved and pleiotropic nature of many genes instrumental to eye development, degeneration might be expected to follow consistent evolutionary trajectories in closely-related animals. We tested this in a comparative study of ocular anatomy in solariellid snails from deep and shallow marine habitats using morphological, histological and tomographic techniques, contextualised phylogenetically. Of 67 species studied, fifteen lack retinal pigmentation and at least seven have eyes enveloped by surrounding epithelium. Independent instances of reduction follow numerous different morphological trajectories. We estimate eye loss has evolved at least seven times within Solariellidae, in at least three different ways: characters such as pigmentation loss, obstruction of eye aperture and 'lens' degeneration can occur in any order. In one instance, two morphologically distinct reduction pathways appear within a single genus, *Bathymophila*. Even amongst closely related animals living at similar depths and presumably with similar selective pressures, the processes leading to eye loss have more evolutionary plasticity than previously realised. Although there is selective pressure driving eye reduction, it is clearly not morphologically or developmentally constrained as has been suggested by previous studies.

Key words: eye degeneration; vision; Solariellidae; deep sea

Introduction

The reduction or loss of eyes is a common feature of animals that inhabit dark environments. This strong evolutionary pattern is found in vertebrates and invertebrates, in lifestyles that range from fossorial (e.g. Borghi et al. 2002) to cavernicolous (e.g. Sadoglu 1967) to abyssal (e.g. Hessler and

Thistle 1975). The evolutionary mechanisms underlying eye loss have been the subject of debate since Darwin postulated that it could be attributed 'wholly to disuse' (1859; Rétaux and Casane 2013). In modern terms, this could be articulated as a release of stabilising selective pressure on, and the subsequent accumulation of mutations in, genes involved in eye development and function (Fong et al. 1995). However, evolutionary experiments have since demonstrated that there is considerable directional selective pressure favouring eye loss in dark environments, for reasons of energetic economy or reinvestment in other sensory systems (Jones and Culver 1989; Yamamoto et al. 2004; Protas et al. 2007; Niven and Laughlin 2008). A particularly interesting emergent question is whether there is a common morphological mechanism or pattern to this process, or if it is driven randomly by neutral mutation or pleiotropy (Rétaux and Casane 2013). Eyes are likely to have evolved more than 40 times among animals and take many different forms (von Salvini-Plawen and Mayr 1977). Within most metazoan clades the basic structure of the eye is broadly conserved, such as vertebrate camera eyes, arthropod apposition or superposition compound eyes, and photosensitive light-spots in planarians. In addition, physical optical constraint combined with evolutionary drive for high-quality vision has resulted in the convergent evolution of the camera eye in both vertebrates and cephalopods. A similarly convergent or restricted process led by morphological or developmental constraint might be expected where structurally similar eyes are lost.

Combined with a selective pressure in favour of eye loss, such evolutionary constraints could determine a most likely order of specific anatomical reduction events. Many authors have described groups of closely-related organisms that have evolved convergent reduced or degenerate eye morphologies, characteristically including size reduction, loss of pigmentation, the envelopment of the eyes by the surrounding tissue, and degeneration of the optic nerve (Langecker

and Longley 1993; Wilkens 2001; Wilkens and Strecker 2003; Protas et al. 2011). Although there is apparently selective pressure for eye loss, additional processes (drift, pleiotropy) are also doubtless implicated in its evolution: some authors have found evidence for a significant role played by the release of evolutionary constraint and subsequent neutral evolution in variety in the loss of eyes at both molecular and morphological levels (Niemiller et al. 2013). Thus, although there are common phenotypic changes which occur during eye reduction, some work has suggested that the specific order of their appearance is not predictable (Poulson 1963). But in other cases it appears that these characters evolve in the same way within groups, and as a result several authors have implied that the process of eye reduction is successive or predictable (Zharkova 1970; Brinton 1987; Wilkens 2001; Jäger 2012; Malkowsky and Götze 2014). This could have a developmental cause. Given the pleiotropic and highly conserved nature of many genes involved in vision and eye structure, certain loci may be targeted during eye reduction (e.g. Jeffery 2009). For example, the developmentally important *Hedgehog* appears to be repeatedly affected both within and between study systems (Leys et al. 2005; Protas et al. 2005; Aspiras et al. 2012). The majority of detailed work on the mechanisms of eye loss to date have used the cave fish *Astyanax mexicanus*, and further studies of eye reduction across a broader taxonomic range of dark-living species are needed to address this question (Malkowsky and Götze 2014). Several other cases of so-called regressive evolution have been similarly examined, such as limb loss in tetrapods and flight loss in ratites, which are both thought to have evolved independently in the same way multiple times (Lande 1978; Baker et al. 2014), but also the loss of the swim bladder in fishes, which has evolved in a more variable fashion (McCune and Carlson 2004). A macroscopic study of the morphological features of eye reduction across a relatively broad group of taxa has not been

undertaken until now, and although there are authors who have acknowledged a need for such a study (e.g. Malkowsky and Götze 2014), none so far have addressed it directly.

To test the extent to which eye reduction is a strictly constrained process requires a group of animals with relatively simple eye structure in which eye loss or reduction has evolved numerous times in closely-related taxa, acting as a 'natural experiment' (Harvey and Pagel 1991). Solariellidae is a family of small marine vetigastropods found worldwide from littoral to abyssal depths, and eye loss has been reported in several species across the family (Marshall 1999; Williams et al. 2013). This group provides an excellent opportunity to study the potential for anatomical determinism in eye loss and to draw comparisons among eyeless taxa, and offers a larger sample of eye reduction events than more commonly-studied cavernicolous groups (Jeffery 2005; Tierney et al. 2015). Vetigastropods typically possess pigment cup eyes (Haszprunar 1988; Ponder and Lindberg 1997; Sasaki 1998; Kano and Kase 2002; Figure 1). The retina consists of apically pigmented cells interspersed with rhabdomeric photoreceptors bearing microvilli and ciliary projections, and the basal side is surrounded by nerve tissue. The eye remains narrowly open, without a cornea, and a vitreous body fills the remainder of the cup and acts as a lens (Ponder and Lindberg 1997; Sasaki 1998). The phylogeny of the solariellids has been resolved by Williams et al. (2013), though here we expand upon that analysis with several new taxa. By comparing the microanatomy of solariellid eyes in a phylogenetic context we can infer the order of reductive elements and compare the anatomical pathways by which eye reduction occurs.

Material and methods

Taxon selection

Sixty-seven species from across Solariellidae were selected for examination of gross eye morphology on the basis of depth, locality and taxonomic position in order to cover a broad range in these fields. These represented 12 of the 14 accepted genera in Solariellidae, as well as one additional undescribed genus, and 67 of an estimated 250 species in the family. One of the non-included genera, *Lamellitrochus*, is likely to be a synonym of *Zetela*, which was represented herein by four other species (Williams et al. 2013). Nine species, including three lacking pigmented eyes, were then selected for histological study to examine the nature and extent of eye reduction, if present. Specimens used for histological study were selected for their tissue quality, as well as to give a good taxonomic and ecological range. A number of undescribed species within the group are noted with the genus name and a numeral following the identifications of Williams et al. (2013). Since Williams et al. (2013) Clades A and C have been formally described as the genera *Arxellia* and *Elaphriella* respectively, and several new species described (Vilvens et al. 2014; Vilvens and Williams 2016). We use the new names in this study. The shallow water species *Ilanga* 6 was included to give a model for comparison to the eyes of several deep-water species: *Elaphriella khantaros*, *Elaphriella wareni*, *Bathymophila diadema*, '*Bathymophila'* 18, *Zetela* 1 and *Zetela alphonsi*. We also included two species from intermediate depths, *Ilanga* 10 and *Spectamen mutabilis* (Williams et al. 2013). These were all found to belong to well-resolved clades by Williams et al. (2013), excepting '*Bathymophila'* 18 and *Zetela alphonsi* which were not included in that study. Preservation of *Z. alphonsi* precluded its inclusion in molecular analyses.

Laboratory methods, sequence editing and alignment

We followed the protocols of Williams et al. (2013) to extract DNA and amplify and sequence portions of the nuclear 28S rRNA gene (28S) and three mitochondrial genes: cytochrome oxidase

subunit I (COI), 16S rRNA (16S) and 12S rRNA (12S). A total of 123 new sequences were added to a subset of previously published sequences for solariellids and five outgroup taxa from appropriate vetigastropod clades (three in Calliostomatidae and two Trochidae) from Williams (2012) and Williams et al. (2013) (new EMBL accession numbers in Table 1, SD6).

Alignments were made in Geneious (v.6.1.7, Kearse et al. 2012), starting with Geneious own alignment and then refined using default settings in Muscle (Edgar 2004) and ClustalW (Larkin et al. 2002) plugins within Geneious. Poorly aligned sites in rRNA alignments were identified using Gblocks Server (0.91b, Castresana 2000) and excluded from analyses. Parameters used in Gblocks allowed for smaller final blocks, gap positions within the final blocks and less strict flanking positions.

Phylogenetic and ancestral state reconstruction

Bayesian phylogenies were determined using MrBayes (v.3.2.2, Huelsenbeck and Ronquist 2001) following the protocol used in Williams et al. (2013) and run on the CIPRES portal (Miller et al. 2010). The best nucleotide substitution models were determined to be GTR+G for 28S and 16S and HKY+I+G for COI and 12S using Akaike Information Criterion (AIC) calculated with jModelTest (Guindon and Gascuel 2003; Darriba et al. 2012). Analyses were run for 20,000,000 generations with a sample frequency of 1,000 in two independent runs. The first ten percent were discarded, so that the final tree was computed from a total of 36,000 trees. Stationarity and convergence between the two runs were determined by examining the potential scale reduction factors (PSRF), standard deviation of split frequencies and by visual examination of .p files in Tracer (v. 1.5; available from http://beast.bio.ed.ac.uk/Tracer).

A combined gene tree was produced in MrBayes including up to three specimens per species for species in the tree published in Williams et al. (2013), plus all available specimens for new taxa, where specimens have sequences for 28S plus at least two mitochondrial genes. Exceptions to this rule were made for three species missing data, as they were the only representatives of new species: *Solariella affinis* (NHMUK 20120233), *Solariella* 6 (MNHN IM-2007-18537) and *Bathymophila* 21 (MNHN IM-2009-15206). Single gene trees for 12S and COI were also produced to confirm species identifications for some specimens not included in the combined gene tree.

We used BEAST (v.1.8.3; Drummond et al. 2012) to analyse molecular data incorporating fossil calibrations. We used the combined gene dataset, but pruned replicate taxa, so that each species was represented by a single specimen sequence. We unlinked all clocks and substitution rates, but linked trees for all four genes. Three monophyletic taxon sets were defined: ingroup (starting age 75 Ma), *Solariella* (starting age 25 Ma) and *Zetela* (starting age 20 Ma), and analyses were performed without including any outgroup sequences. These groups follow the same constraints and fossil calibrations used in Williams et al. (2013). The ingroup was constrained to be at least 71 Ma (95% interval: 71.4–89 Ma; mean in real space: 4.18, log stdev: 1, offset: 71). The *Solariella* clade was constrained to be at least 23 Ma (95% interval: 23.2–34 Ma; mean in real space: 2.555, log stdev: 1, offset: 23). The *Zetela* clade was constrained to be at least 16.7 Ma (95% interval: 16.7–27.9 Ma; mean in real space: 2.65, log stdev: 1, offset: 16.5) (see Williams et al. 2013 for justification of fossil choices). Nucleotide substitution models were those chosen by jModelTest, except the model for 16S which was simplified to HKY+G after preliminary runs. Uncorrelated relaxed, lognormal clocks were used for all genes, with a birth-death speciation prior and a random

starting tree. We used a diffuse gamma distribution (shape 0.001, scale 1000) for the ucld.mean parameters. The analysis ran for 100,000,000 generations with trees sampled every 10,000 steps.

Additional supporting phylogenetic analyses under parsimony were run in POY (Varón et al. 2010) using the same sequence data. Analyses used incongruent length difference parameter set 141 (with a simulated cost ratio of indel:transversion:transition of 1:4:1) for all sequences and were run for 30,000,000 generations with a sample frequency of 1 tree per 1,000. The first 25% of trees were discarded, so that the final consensus tree was computed from a total of 22,500 trees.

Ancestral state reconstructions for eye characters were performed in Mesquite (Maddison and Maddison 2015) using parsimony and Maximum Likelihood to calculate most parsimonious character states and proportional likelihoods for character states at each node of the time-calibrated tree produced in BEAST. Likelihood ratio testing indicated that single rate Markov (Mk1) models provided the best fit for eye pigmentation, size and status of the vitreous body, and that a two-rate asymmetric model (Mk2) was more appropriate for the status of the eye aperture in Maximum Likelihood reconstructions.

Gross morphology

We examined 114 individual specimens of 67 different species (Table 1) using as many deep-sea species as possible from across the family; all available genera were sampled (see above for taxon selection). Non-destructive examinations of the eyes under a dissecting microscope were sufficient to determine the presence or absence of pigment and, where pigment was present, the status of the eye aperture and any tissue obscuring it. These two characters were used as broad indicators of eye loss so as to track its presence throughout the family.

Histology and digital reconstruction

198 The left eye and surrounding tissue was removed from the nine specimens selected for histological
199 studies. For material stored in ethanol (all specimens except *Zetela alphonsi*), tissue required
200 gradual re-hydration through a decreasing ethanol series (3 x 15 minutes in 90%, 70%, 50%, and
201 30% ethanol and pure distilled water). Samples were post-fixed in 1% osmium tetroxide in distilled
202 water for 2 hours, washed in distilled water and dehydrated in an increasing acetone series. The
203 specimen of *Z. alphonsi* was fixed in 2.5% glutaraldehyde in cacodylate buffer (0.1 M, pH 7.4),
204 osmicated in 1% osmium tetroxide in cacodylate buffer, washed in dilute cacodylate buffer, and
205 dehydrated in acetone as before, after Ruthensteiner (2008). Tissue was embedded in Epon epoxy
206 resin with DPM-30 accelerator for 48 hours at 65°C, according to the manufacturer's instructions
207 (Sigma Life Sciences).

208 Samples were serially sectioned at a thickness of 1.5 µm using a diamond knife (HistoJumbo 8mm,
209 DiATOME 8mm, Switzerland) on an automated microtome (Leica RM2255) and stained using
210 Richardson's solution (Richardson et al. 1960). Images of sections were digitally recorded using
211 an Olympus E-600 digital camera mounted on an Olympus BX41 light microscope at a
212 magnification appropriate to each sample. The images were reduced and contrast-enhanced for
213 reconstruction using Adobe Photoshop CS4. Images were aligned into stacks using AMIRA v5.3.3
214 (Visualisation Sciences Group) and anatomical features of the eye were identified throughout the
215 image stacks before surface rendering and smoothing to produce 3D tomographic models.

216

Results

Eye reduction was evident in 20 of the 67 species studied overall. Morphological changes observed through gross morphology and histology included loss of pigmentation, obstruction of the eye aperture, reduction or fragmentation of the vitreous body, and overall reduction in eye size. In the context of the phylogenetic reconstruction we estimate that eye reduction has evolved at least seven times (and in at least seven genera) in Solariellidae, along variable morphological pathways.

Phylogenetic and ancestral state reconstruction

A time-calibrated combined-gene tree generated in BEAST resolved clear genus-level clades with generally high support, and we present it here as a fully-resolved tree (Figure 4). The topology is similar to that resolved by Williams et al. (2013): the same ten clades corresponding to genera were also recovered in this study, along with , *Microgaza rotella*, a genus not represented in the previous study, and '*Bathymophila'* 18, which falls outside *Bathymophila* despite appearing morphologically to belong therein. As in Williams et al. (2013) '*Suavotrochus'* sp. and '*Machaeroplax' delicatus* do not resolve within any of these genus-level clades. Relationships among clades generally had high statistical support (node support values greater than 70% for all but one relevant node). There were two key topological differences from previous analyses by Williams et al.: the placement of (*Archiminolia+Arxellia*) in a larger grouping (*Bathymophila*+('*Bathymophila'* 18+ (*Archiminolia+Arxellia*)), though this is not well supported (Figure 4), and the non-recovery of a clade ((*Zetela*+Clade B)+(*Minolia+Hazuregyra watanabei*)), which was only poorly supported in Williams et al. (2013). Within-clade (species level) relationships are almost identical to those resolved by Williams et al. (2013) where sampling is consistent with that study. The combined-gene trees produced in MrBayes (SD1) showed well-

resolved generic-level clades in agreement with previous results (Williams et al. 2013), which further support the combined-gene BEAST analysis. In Bayesian analyses under MrBayes, within-clade relationships were identical except for the relative positions of *Spectamen mutabilis* and *Spectamen laevior*. Relationships between clades were not well resolved. The *Ilanga* and (*Elaphriella*+(*Machaeroplax*+*Suavotrochus*)) clades were resolved as the two earliest diverging groups, but MrBayes analyses recovered separate Clade B and *Zetela* groups diverging next (though with lower support than the alternative relationships found in BEAST) (SD1). Individual gene trees clearly resolved species-level clades (SD2,3)

In MrBayes analyses the average standard deviation of split frequencies approached zero, all parameter average PSRF values were ≤ 1.003 and in these Bayesian analyses minimum ESS values in combined runs exceeded 200 for all parameters. Visual examination of traces showed that all parameters reached stationarity and converged between independent runs for each dataset.

Parsimony analyses further support the BEAST and MrBayes trees, and no additional information regarding topology was recovered. In line with the previous work of Williams et al. (2013), we therefore illustrate the results of BEAST analyses as our preferred tree and the basis of further inference (Figure 4).

Within-clade relationships and several between-clade relationships were particularly well supported by consensus across all analyses and methods, such as the groupings of *Solariella* and *Spectamen*, *Arxellia*, *Archiminolia* and *'Bathymophila'* 18, and *Microgaza*, *Minolia* and *Hazuregyra.* Where topological conflicts occurred we referred to the better-supported higher level topology resolved by the BEAST tree to generate ancestral state reconstructions for assigned eye characters (SD4).

Gross morphology

Solariellids fall into three distinct groups of eye morphs (Figure 2, 3). Of the 67 species studied, 47 have typical pigmented eyes of normal size with an open aperture, and at least one of these morphs were found in all genera examined, except in *Machaeroplax* and *Suavotrochus* (Figure 4, Table 1). Fifteen species across at least seven genera (*Archiminolia, Elaphriella, Suavotrochus, Machaeroplax, Zetela, Bathymophila* and '*Bathymophila'* 18; generic level placement of the latter is uncertain) lack pigmented eyes (Figure 4, Table 1). The status of the eye aperture and size of the eye are not visible in these specimens without histology. Five species in two genera (*Bathymophila* and *Elaphriella*) retain their pigmentation but the eye aperture is obscured by a layer of tissue covering the eye, which is of a normal size (Figure 4, Table 1). One species, *Zetela* 1, has unusual eyes of which the proximal half is pigmented and the distal half is not, so the aperture (if present) is not visible. This was observed in all three specimens studied. In the context of our phylogenetic and ancestral state reconstructions, we conclude that eye reduction (the novel appearance of one or more reduced characters in a previously fully-eyed lineage) has evolved at least seven times independently in Solariellidae; at least twice in *Bathymophila* (*sensu* Williams et al. 2013), and at least once in each of *Archiminolia, Elaphriella, Zetela*, and (*Machaeroplax* + *Suavotrochus*) (Figure 4).

Histology and digital reconstruction

Among the nine species studied histologically, we identified five different eye anatomies. Structurally typical vetigastropod eyes were confirmed in three species: *Ilanga* 6, *Ilanga* 10 and *Spectamen mutabilis* all have fully formed pigmented eyes on short eyestalks posterior of the base of the cephalic tentacle (Figure 2). The vitreous body is large, round and intact, microvilli are

well organised and of uniform length, and photoreceptors are interspersed between the pigment cells of the retina (Figure 3A, SD5.1, SD5.2, SD5.3). The eye aperture is open and unobstructed, and the optic nerve can be traced from the retina to the cerebral ganglion. There are minor anatomical differences between these three species; the eye of *Ilanga* 10 appears to be slightly compressed with microvilli of variable lengths, and the eye of *S. mutabilis* has an unusually wide aperture (53 µm, eye diameter 85 µm), the vitreous body is slightly reduced in size and microvilli are very long.

A layer of tissue covers the eye in two species: *Bathymophila diadema* and *Elaphriella khantaros* (Figure 3B, SD5.4). A layer of external epithelium, the closed retinal epithelium and, in all but a very small central area, some interstitial tissue cover the eye and obstruct the aperture. In this central area, the retina passes very close to the surface epithelium and may fuse with it, but there is no opening (Figure 3B). In both species, the retina is pigmented and cells are well-organised, with many photoreceptors and a strong connection to the optic nerve (Figure 3B, SD5.4). Again, there are obvious differences between the two species. There appears to be less pigmentation in the retina of *B. diadema* than in other species (e.g. *Ilanga,* Figure 3B) and the vitreous body, though present, is small and fragmented and microvilli are elongated. Some of the optic cup appears to be empty (Figure 3B). In *Elaphriella khantaros* the vitreous body is large and intact and microvilli are irregular lengths.

Reduced eyes, which were invisible from the surface due to loss of pigmentation, were found in '*Bathymophila'* 18 (Figure 3D, SD5.5). The vitreous body is fragmented and reduced, and few ciliary photoreceptors are visible. The eye of '*Bathymophila'* 18 was very small (diameter 55 µm, body length 5 mm), with the retina only counting 14 cells across at its widest point, whereas the smallest specimen overall, *Spectamen mutabilis* (body length 4 mm), had a retina at least 22 cells

across (eye diameter 85 µm). The eye aperture appeared to remain open and uncovered in both species, but was very narrow (5 µm) in *'Bathymophila'* 18 (Figure 3D) compared to the more typical eyes of *Ilanga* 6 (aperture 70 µm, eye diameter 250 µm). The eye remains well connected to the optic nerve, which is large and reaches the cerebral ganglion intact (SD5.5).

Unpigmented eyes were also observed in *Elaphriella wareni* and *Zetela alphonsi*, but in these species the eye aperture was covered by a layer of tissue in a fashion reminiscent of *Bathymophila diadema* and *Elaphriella khantaros* (Figure 3C, SD5.6). In addition, the vitreous body appears to be entirely absent in *E. wareni*, and microvilli are elongated and irregular. Some ciliary projections of photoreceptors are present. The optic nerve surrounds the optic cup and is larger at the distal (eye) end; it connects to the cerebral ganglion as in other species but it narrows considerably towards the proximal (brain) end (Figure 3C, SD5.6).

Partially-pigmented but apparently misshapen eyes were found in *Zetela* 1. This species has straight, slender eyestalks with the eye protruding from the tip (Figure 2D). The eye does not represent the typical cup shape observed in other species, instead being ball-shaped and without an aperture, and not surrounded by other tissue (nerve tissue is only visible at the very base) (SD5.7). The proximal part of the retina is pigmented, but the distal side is not. Modelling revealed a dent-like disfigurement in the shape of the eye, which was also seen, but to a lesser extent, in the other specimens of the same species (SD5.7). The vitreous body was visible in few sections and appears to be small, with a large volume of long microvilli filling the proximal part of the eye and a large part of the distal side being empty (SD5.7).

Discussion

The number and variability of eye reductions found within Solariellidae indicate that although there is evidence of strong selective pressure in favour of eye loss in dark-living animals (Jones and Culver 1989), the anatomical trajectory of its evolution is not predictable or consistent even amongst closely related species. These findings have important implications for understanding the biology of this gastropod family but also as a case study for the evolution of the loss of complex traits such as eyes (Serb and Eernisse 2008).

Eye loss and evolution in Solariellidae

Eye reduction is more widespread than previously reported amongst deep-sea solariellids, and we documented many new cases here (Williams et al. 2013). The frequency of apparently independent eye reduction and loss events with variable anatomical forms has positioned Solariellidae as an important group for the study of 'reductive' evolution. The group contains many undescribed species and more continue to be discovered (Marshall 1999; Vilvens 2002; Williams et al. 2013; Vilvens et al. 2014; Vilvens and Williams 2016). As well as recording the presence or absence of retinal pigmentation in additional species, we also introduced a new metric, the presence or absence of the eye aperture, which can in many cases be determined without invasive examination. Combined with pigmentation data, this indicated that eye reduction is much more widespread than previously reported, occurring in at least six of the fourteen solariellid genera (the placement of '*Bathymophila'* 18 is unclear; Figure 4). Even in groups beyond Vetigastropoda where there is no exposed eye aperture, the use of covering or sinking of the eye itself can be used as a comparable

metric for eye reduction. The lack of pigmentation in the retina of *Archiminolia oleacea* is unusual, as it mostly inhabits intermediate depths and this feature has not been reported previously, though it has potential taxonomic importance because *A. oleacea* is the type species of the genus. Both *A. oleacea* and *Zetela alphonsi* may be unique in their genera for lacking retinal pigmentation, with congeneric species descriptions either noting the presence of pigmented eyes, or omitting description of the eyes altogether. In *Bathymophila* it is possible that the loss of eyes in both clades coincided with their rapid diversification after expansion into deeper water as suggested by Williams et al. (2013). Similar increases in diversification rate have been observed in eyeless deep-water clades of ostracods, compared to sighted shallow-water clades (Syme and Oakley 2012). Conversely, some deep-sea species in this family appear to have retained intact eyes despite a substantial evolutionary history of inhabiting deep water, such as *Bathymophila* 21 and Clade B sp.2 (Williams et al. 2013). Further investigation of ocular ultrastructure in more species, especially those with apparently degenerate eyes (*Bathymophila* spp., *A. oleacea, E. paulinae, Suavotrochus, Machaeroplax*) is warranted to determine whether they show other signs of eye reduction as well. The status of characters such as the eye aperture can only be determined through histological sampling.

Most importantly, this study demonstrates that the evolutionary route to eye loss is highly variable even among these closely related species. Reduction events such as loss of pigmentation, degradation of the 'lens' and covering of the eye aperture can occur independently. This is strong evidence that such individual features do not appear in any particular order in a trajectory towards eye loss. While the eyes of some species (*Bathymophila diadema, Elaphriella khantaros*) have become enveloped by the surrounding epithelium, they retain their retinal pigmentation. Conversely, others have non-pigmented eyes that remain unobstructed (*'Bathymophila'* 18).

373 Degeneration of the vitreous body has occurred in some, but not all, otherwise apparently similar
374 eye morphs (*Bathymophila diadema* has a fragmented vitreous body but *Elaphriella khantaros*
375 does not), and overall reduction in size is observed in only one species (*'Bathymophila'* 18). Our
376 ancestral state reconstructions support this conclusion and indicate that the features we have
377 identified can occur in different orders. Further additions to our histological dataset will help to
378 clarify the evolutionary history of these traits and further reduce uncertainty in the character
379 reconstruction. It is clear from the data presented here that even in closely-related species there is
380 no evidence for a consistent order of events. This is demonstrated not only by the fundamentally
381 different structural changes which have occurred in *Elaphriella khantaros* and *'Bathymophila'* 18,
382 for example, but also by the two contrasting morphologies within *Bathymophila* (*sensu* Williams
383 et al. 2013) despite their taxonomic proximity (Figure 3, 4).Without secondary regain of features,
384 which we consider to be unlikely, these different morphological pathways are simply mutually
385 exclusive. Additionally, this conclusion is also robust to any remaining phylogenetic uncertainty
386 in the fully resolved BEAST tree: we have confirmed species identity of all specimens (SD2,3)
387 and recovered relationships within clades which are supported by previous and supporting analyses
388 (SD1; Williams et al. 2013). The key anatomical divergences that support our conclusion are found
389 at taxonomic levels unaffected by phylogenetic uncertainty at deeper nodes.

390 *Broader implications for the evolution of eye loss*

391 The variety in evolutionary trajectory apparent in Solariellidae indicates there is unlikely to be a
392 universal developmental cause of eye reduction, even between closely related species. Studies
393 of the cavefish *Astyanax mexicanus* have shown that the lens, and the apoptosis of cells therein,
394 controls subsequent degeneration events, resulting in many of the convergent morphological
395 features seen in independent eyeless populations (Jeffery 2005). Alterations to lens apoptosis

during development are also implicated in the eye degeneration of two *Rhamdia* cave catfishes (Wilkens 2001). However, given the variety of pathways to reduction found in solariellids, it is unlikely that there is a similar developmental 'master key' that affects eye development downstream in this group. In the future, we propose that visual anatomy in Solariellidae or other gastropod or molluscan groups could provide valuable new model systems for wider evolutionary studies (Serb and Eernisse 2008).

Histological investigations show structural features that deviate from the 'typical' solariellid eye in seven of nine species examined, which in many cases were not visible from superficial examinations. Not only the loss of pigmentation, but the covering of the eye by epithelial tissue, disintegration of the vitreous body and reduction in size are all classic characters associated with eye reduction in dark environments (Culver 1982). The elongation of microvilli and widened aperture seen in *Spectamen mutabilis* may contribute to increasing light capture and heightening visual sensitivity in dim, intermediate-depth environments (Warrant et al. 2003; Land and Nilsson 2012; Malkowsky and Götze 2014).

There are of course typical character states which are found at some stage during the evolution of eye loss in this case: loss of pigmentation, disintegration of the vitreous body and covering of the eye have evolved recurrently in taxa undergoing eye reduction independently. This trend is well-known and extends beyond the taxonomic scope of this study; these same reduction events have been reported in many other animal groups (Culver 1982; Jones et al. 1992). However, by atomising the overall process of eye loss, we found that the order of their occurrence is not consistent and thus individual 'reduced' phenotypes can be very different. Pigmentation is not the ultimate indicator of eye function, though it has been used as such a proxy for many years. Here we have shown that many species deviate significantly from the typical form without losing

pigmentation, and this suggests that similar cases may have been missed in other groups. By mapping anatomical data on our resolved tree, it is clear that the reduction of specific anatomical features represent different processes taking place in parallel, and thus the presence or absence of pigmentation does not necessarily reflect other aspects of eye structure (Figure 4). Histological studies, though time consuming, are necessary to properly understand what is happening beneath the surface. Certain characteristic features of reduction that we expected to observe do not appear to have occurred at all, including degeneration of the nerve tissue. Although this is considered a classic sign of eye redundancy (Culver 1982; Langecker and Longley 1993), the absence of neural degeneration has also been observed in blind cave fishes (Wilkens and Strecker 2003) and it has been suggested that dysfunctional eyes could be adapted or modified to detect other stimuli such as chemical cues, accounting for the persistence of the optic nerves (Brinton 1987).

Indeed, the putative potential for energetic reinvestment in other sensory systems is one possible evolutionary advantage of eye reduction: as well as losing their eyes, many cave animals have elongated limbs and antennae, and increased sensitivity to tactile and chemical cues (Culver 1982; Iliffe and Kornicker 2009). In the case of solariellids and other vetigastropods, a pair of cephalic tentacles originate from the head from the same point as the eyestalks, with paired accessory tentacles posterior and usually ventral to this. These cephalic tentacles are often thicker in deeper-water solariellid taxa (STW, pers. obs.). More detailed examination of these tentacles and their innervation may shed some light on the relative investment balance between vision and mechano- or chemoreception in the tentacles. Given the intermediate state of eye loss observed in several species, this could help determine whether the eyes themselves are still functional in any rudimentary way or whether an energetic trade-off is occurring, in the absence of live observations. However Culver et al. (1995) suggest that these ‘constructive’ traits may arise more slowly than

the ‘regressive’ loss of eyes as a result of the faster action of combined neutral evolution and selection on eye-related genes compared to selective pressure alone on other sensory modalities, and we did not observe any dramatic differences in tentacle morphology between eyed and eyeless species.

Where eye reduction evidentially has evolved in very different ways, it is possible that other evolutionary constraints affect its trajectory. In talpid moles, for example, eye reduction is thought to have been significantly influenced by ecology and biomechanics of burrowing techniques (Borghi et al. 2002). Some deep-sea fishes with overlapping depth ranges exhibit different extents of eye degeneration, also likely as a result of different ecological pressures and behaviour (Munk 1964). Depth does appear to be a fairly good indicator for eye reduction overall in the current study, with only four of the twenty deep-water species (600 metres and deeper) apparently having typical eyes, but several species inhabiting similar depths and regions differ dramatically in their eye structure. This also includes *Archiminolia oleacea* and *Bathymophila* 9, which exhibit pigment loss even at shallow depths (though this is likely to be ancestral to the *Bathymophila* clade). Ecological or behavioural differences such as feeding habits, major predators or residual eye functionality may wholly or partially account for some of these variations, but due to the rarity and inaccessibility of these species and the absence of live observations, we lack further data that may be necessary to take into account.

Both directional selection and neutral mutation have important roles to play in the evolution of eye loss, with the former apparently driving for the reduction of eyes overall (Jones and Culver 1989), and the latter, or a combination of the two, likely generating the random order of reduction events which we see here (Fong et al. 1995; Wiens et al. 2003); however disentangling their relative contributions remains a considerable challenge. Although evolutionary process cannot be directly

inferred from the patterns we observe here, they appear to be congruent with a significant role for the release of evolutionary constraint. Our findings do emphasise the importance of terminology regarding regressive evolution; many authors describe ‘convergent evolution’ of eye reduction in dark-dwelling species (e.g. Derkarabetian et al. 2010; Hedin and Thomas 2010). However, although the reduction of eyes occurs frequently, it appears that both the evolutionary mechanisms by which it evolves and the resulting anatomy are not necessarily convergent. It is important to distinguish between the process and the resulting character, as this affects the implications of interplay between selection, neutral mutation and pleiotropy. For example Brinton (1987) and Zharkova (1970) described four stages of eye loss in deep-sea crustaceans, Jäger (2012) discovered several species of troglobitic spider which displayed ‘gradually increasing troglomorphic features’, and Malkowsky and Götze (2014) found convergent patterns in the eye structure of scallops living in aphotic zones and referred to the evolution of eye reduction in this case as ‘successive’. However, these studies did not consider the overlap of occurrence of specific reduction features, despite implying predictability in their results. These systems represent untested hypotheses, where phylogeography could be compared to anatomy to determine whether there is or is not a conserved anatomical trajectory to eye reduction.

Conclusions

This study was restricted to a single family and compared closely related species. Many of them overlap geographically and in depth range, and are potentially exposed to comparable selective pressures. One might expect their identical conditions, simple and well-conserved eye structure and shared morphological constraints to have produced similar reduced eye morphologies. However, we found evidence against a conserved pathway for eye reduction, with dramatic

differences in reduction morphology occurring even within a single genus. There is greater plasticity in this process than has previously been appreciated, and we consider it highly unlikely that eye loss occurs through a common or most likely morphological trajectory, certainly within Mollusca and most likely throughout Metazoa.

Acknowledgements

We gratefully acknowledge Philippe Bouchet (MNHN), who kindly provided many of the specimens used in this study. MNHN material was collected during expeditions of the 'Tropical Deep-Sea Benthos' programme under PIs Bertrand Richer de Forges, Philippe Bouchet, and Sarah Samadi: AURORA, BENTHAUS, BERYX, BIOPAPUA, BOA 1, BORDEAU 1, CONCALIS, EBISCO, NORFOLK 1 and 2, PANGLAO 2005, SOLOMON 1 and 2, TAIWAN 2001, and TERRASSES. The Principal Investigators acknowledge Institut de Recherche pour le Développement (IRD), the Philippines Bureau of Fisheries and Aquatic Resources (BFAR), and National Taiwan Ocean University (NTOU) for ship time. Additional material was collected during the MNHN-PNI 'Our Planet Reviewed' expeditions: MAINBAZA, MIRIKY, PANGLAO 2004, and SANTO 2006, for which Philippe Bouchet acknowledges the support of the Total Foundation and Prince Albert II of Monaco Foundation. For the context of the expeditions, see Bouchet et al. (2008) and http://expeditions.mnhn.fr/?lang=en_US. We also thank Enrico Schwabe and Martin Heβ (ZSM, LMU) for discussions leading to the design of this project and for the use of specimens of *Zetela alphonsi*, Bruce Marshall (NMNZ) for his assistance with specimens of *Archiminolia oleacea*, Jessica Sells (NHM) for her assistance in the laboratory and the staff of Queen's University Marine Laboratory (QUB) for their technical assistance. We are also very grateful for the valuable comments and feedback of three reviewers.

511 *References*

512 Aspiras, A. C., R. Prasad, D. W. Fong, D. B. Carlini, and D. R. Angelini. 2012. Parallel reduction
513 in expression of the eye development gene *hedgehog* in separately derived cave populations of the
514 amphipod *Gammarus minus*. J. Evol. Biol. 25:995–1001.

515 Baker, A. J., O. Haddrath, J. D. McPherson, and A. Cloutier. 2014. Genomic support for a Moa-
516 Tinamou clade and adaptive morphological convergence in flightless ratites. Mol. Biol. Evol. 1–
517 11.

518 Borghi, C. E., S. M. Giannoni, and V. G. Roig. 2002. Eye reduction in subterranean mammals and
519 eye protective behaviour in *Ctenomys*. Mastozoología Neotrop. J. Neotrop. Mammal. 9:123–134.

520 Brinton, E. 1987. A new abyssal Euphausiid, *Thysanopoda minyops*, with comparisons of eye size,
521 photophores, and associated structures among deep-living species. 7:636–666.

522 Castresana, J. 2000. Selection of conserved blocks from multiple alignments for their use in
523 phylogenetic analysis. Mol. Biol. Evol. 17:540–552.

524 Culver, D. C. 1982. Cave Life: Evolution and Ecology. Harvard University Press.

525 Culver, D. C., T. C. Kane, and D. W. Fong. 1995. Adaptation and natural selection in caves: The
526 evolution of *Gammarus minus*. Harvard University Press, Cambridge, MA.

527 Darriba, D., G. L. Taboada, R. Doallo, and D. Posada. 2012. jModelTest 2: more models, new
528 heuristics and parallel computing. Nat. Methods 9:772.

529 Darwin, C. 1859. Origin of Species. John Murray, London.

530 Derkarabetian, S., D. B. Steinmann, and M. Hedin. 2010. Repeated and time-correlated
531 morphological convergence in cave-dwelling harvestmen (Opiliones, Laniatores) from Montane
532 Western North America. PLoS One 5:e10388.

Drummond, A. J., M. A. Suchard, D. Xie, and A. Rambaut. 2012. Bayesian phylogenetics with BEAUti and the BEAST 1.7. Mol. Biol. Evol. 29:1969–1973.

Edgar, R. C. 2004. MUSCLE: multiple sequence alignment with high accuracy and high throughput. Nucleic Acids Res. 32:1792–1797.

Fong, D. W., T. C. Kane, and D. C. Culver. 1995. Vestigialisation and loss of non-functional characters. Annu. Rev. Ecol. Syst. 26:249–268.

Guindon, S., and O. Gascuel. 2003. A simple, fast and accurate method to estimate large phylogenies by maximum-likelihood. Syst. Biol. 52:696–704.

Harvey, P. H., and M. D. Pagel. 1991. The comparative method in evolutionary biology. Oxford University Press, Oxford.

Haszprunar, G. 1988. On the origin and evolution of major gastropods group, with special reference to the streptoneura. J. Molluscan Stud. 54:367–441.

Hedin, M., and S. M. Thomas. 2010. Molecular systematics of eastern North American Phalangodidae (Arachnida: Opiliones: Laniatores), demonstrating convergent morphological evolution in caves. Mol. Phylogenet. Evol. 54:107–21.

Hessler, R. R., and D. Thistle. 1975. On the place of origin of deep-sea isopods. Mar. Biol. 32:155–165.

Huelsenbeck, J. P., and F. Ronquist. 2001. MRBAYES: Bayesian inference of phylogenetic trees. Bioinformatics 17:754–755.

Iliffe, T. M., and L. S. Kornicker. 2009. Worldwide diving discoveries of living fossil animals from the depths of anchialine and marine caves. Smithson. Contrib. Mar. Sci. 38:269–280.

Jäger, P. 2012. Revision of the genus *Sinopoda* Jäger, 1999 in Laos with discovery of the first

555 eyeless huntsman spider species (Sparassidae: Heteropodinae). Zootaxa 57:37–57.

556 Jeffery, W. R. 2005. Adaptive evolution of eye degeneration in the mexican blind cavefish. J.
557 Hered. 96:185–196.

558 Jeffery, W. R. 2009. Regressive evolution in *Astyanax* cavefish. Annu. Rev. Genet. 43:25–47.

559 Jones, R., and D. C. Culver. 1989. Evidence for selection on sensory structures in a cave population
560 of *Gammarus minus*. Evolution 43:688–693.

561 Jones, R., D. C. Culver, and T. C. Kane. 1992. Are parallel morphologies of cave organisms the
562 result of similar selection pressures? Soc. Study Evol. 46:353–365.

563 Kano, Y., and T. Kase. 2002. Anatomy and systematics of the submarine-cave gastropod *Pisulina*
564 (Neritopsina: Nertiliidae). J. Molluscan Stud. 68:365–384.

565 Kearse, M., R. Moir, A. Wilson, S. Stones-Havas, M. Cheung, S. Sturrock, S. Buxton, A. Cooper,
566 S. Markowitz, C. Duran, T. Thierer, B. Ashton, P. Mentjies, and A. Drummond. 2012. Geneious
567 Basic: an integrated and extendable desktop software platform for the organization and analysis of
568 sequence data. Bioinformatics 28:1647–1649.

569 Land, M. F., and D.-E. Nilsson. 2012. Animal Eyes. Second. Oxford University Press, Oxford.

570 Lande, R. 1978. Evolutionary mechanisms of limb loss in tetrapods. Evolution 32:73–92.

571 Langecker, T. G., and G. Longley. 1993. Morphological adaptations of the Texas blind catfishes
572 *Trogloglanis pattersoni* and *Satan eurystomus* (Siluriformes: Ictaluridae) to their underground
573 environment. Am. Soc. Icthyologists Herpetol. 1993:976–986.

574 Larkin, M. A., G. Blackshields, N. P. Brown, R. Chenna, P. A. McGettigan, H. McWilliam, F.
575 Valentin, I. M. Wallace, A. Wilm, R. Lopez, J. D. Thompson, T. J. Gibson, and D. Higgins. 2002.
576 ClustalW and ClustalX version 2. Bioinformatics 23:2947–2948.

577 Leys, R., S. J. B. Cooper, U. Strecker, and H. Wilkens. 2005. Regressive evolution of an eye
578 pigment gene in independently evolved eyeless subterranean diving beetles. Biol. Lett. 1:496–9.

579 Maddison, W. P., and D. R. Maddison. 2015. Mesquite: a modular system for evolutionary
580 analysis. Version 3.04.

581 Malkowsky, Y., and M.-C. Götze. 2014. Impact of habitat and life trait on character evolution of
582 pallial eyes in Pectinidae (Mollusca: bivalvia). Org. Divers. Evol., doi: 10.1007/s13127-013-0165-
583 z.

584 Marshall, B. A. 1999. A revision of the recent Solariellinae (Gastropoda: Trochoidea) of the New
585 Zealand region. Nautilus (Philadelphia). 113:4 – 42.

586 McCune, A. R., and R. L. Carlson. 2004. Twenty ways to lose your bladder: common natural
587 mutants in zebrafish and widespread convergence of swim bladder loss among teleost fishes. Evol.
588 Dev. 6:246–259.

589 Miller, M. A., W. Pfeiffer, and T. Schwartz. 2010. Creating the CIPRES Science Gateway for
590 inference of large phylogenetic trees. Pp. 1–8 *in* Proceedings of the Gateway Computing
591 Environments Workshop (GCE). New Orleans.

592 Munk, O. 1964. The eyes of three benthic deep-sea fishes caught at great depths. Galathea Rep.
593 7:137–149.

594 Niemiller, M. L., B. M. Fitzpatrick, P. Shah, L. Schmitz, and T. J. Near. 2013. Evidence for
595 repeated loss of selective constraint in rhodopsin of Amblyopsid cavefishes (Teleosti:
596 Amblyopsidae). Evolution 67:732–748.

597 Niven, J. E., and S. B. Laughlin. 2008. Energy limitation as a selective pressure on the evolution
598 of sensory systems. J. Exp. Biol. 211:1792–1804.

599 Ponder, W. F., and D. R. Lindberg. 1997. Towards a phylogeny of gastropod molluscs: an analysis
600 using morphological characters. Zool. J. Linn. Soc. 119:83–265.

601 Poulson, T. L. 1963. Cave adaptation in amblyopsid fishes. Am. Midl. Nat. 70:257–290.

602 Protas, M., M. Conrad, J. B. Gross, C. Tabin, and R. Borowsky. 2007. Regressive evolution in the
603 mexican cave tetra, *Astyanax mexicanus*. Curr. Biol. 17:452–454.

604 Protas, M. E., C. Hersey, D. Kochanek, Y. Zhou, H. Wilkens, W. R. Jeffery, L. I. Zon, R.
605 Borowsky, and C. J. Tabin. 2005. Genetic analysis of cavefish reveals molecular convergence in
606 the evolution of albinism. Nat. Genet. 38:107–111.

607 Protas, M. E., P. Trontelj, and N. H. Patel. 2011. Genetic basis of eye and pigment loss in the cave
608 crustacean, *Asellus aquaticus*. Proc. Natl. Acad. Sci. U. S. A. 108:5702–7.

609 Rétaux, S., and D. Casane. 2013. Evolution of eye development in the darkness of caves:
610 adaptation, drift, or both? Evodevo 4:26.

611 Richardson, K. C., L. Jarret, and E. H. Finke. 1960. Embedding in epoxy resins for ultrathin
612 sectioning in electron microscopy. Stain Technol. 35:313–323.

613 Ruthensteiner, B. 2008. Soft part 3D visualisation by serial sectioning and computer
614 reconstruction. Zoosymposia 1:63–100.

615 Sadoglu, P. 1967. The selective value of eye and pigment loss in mexican cave fish. Evolution
616 21:541–549.

617 Sasaki, T. 1998. Comparative anatomy and phylogeny of the recent Archaeogastropoda (Mollusca:
618 Gastropoda). Univ. Museum, Univ. Tokyo, Bull. 38:1–223.

619 Serb, J. M., and D. J. Eernisse. 2008. Charting evolution's trajectory: using molluscan eye diversity
620 to understand parallel and convergent evolution. Evol. Educ. Outreach 1:439–447.

621 Syme, A. E., and T. H. Oakley. 2012. Dispersal between shallow and abyssal seas and evolutionary
622 loss and regain of compound eyes in cylindroleberidid ostracods: conflicting conclusions from
623 different comparative methods. Syst. Biol. 61:314–36.

624 Tierney, S. M., S. J. B. Cooper, K. M. Saint, T. Bertozzi, J. Hyde, W. F. Humphreys, A. D. Austin,
625 and S. M. Tierney. 2015. Opsin transcripts of predatory diving beetles : a comparison of surface
626 and subterranean photic niches. R. Soc. Open Sci. 2.

627 Varón, A., L. S. Vinh, and W. C. Wheeler. 2010. POY version 4: phylogenetic analysis using
628 dynamic homologies. Cladistics 26:72–85.

629 Vilvens, C. 2002. Description of *Zetela alphonsi* n.sp. (Gastropoda: Trochidae: Solariellinae) from
630 Chile. Novapex 3:61 – 64.

631 Vilvens, C., and S. T. Williams. 2016. New genus and new species of Solariellidae (Gastropoda:
632 Trochoidea) from New Caledonia, Fiji, Vanuatu, Solomon Islands, Philippines, Papua New
633 Guinea and French Polynesia. Trop. Deep Sea Benthos 28.

634 Vilvens, C., S. T. Williams, and D. G. Herbert. 2014. New genus *Arxellia* with new species of
635 Solariellidae (Gastropoda: Trochoidea) from New Caledonia, Papua New Guinea, Philippines,
636 Western Australia, Vanuatu and Tonga. Zootaxa 3826:255–281.

637 von Salvini-Plawen, L., and E. Mayr. 1977. On the evolution of photoreceptors and eyes. Evol.
638 Biol. 10:207–263.

639 Warrant, E. J., S. P. Collin, and N. A. Locket. 2003. Eye design in deep-sea fishes. Pp. 303–322
640 *in* S. P. Collin and N. J. Marshall, eds. Sensory Processing in Aquatic Environments. Springer,
641 New York.

642 Wiens, J. J., P. T. Chippindale, and D. M. Hillis. 2003. When are phylogenetic analyses misled by

643 convergence? A case study in Texas cave salamanders. Syst. Biol. 52:501–514.

644 Wilkens, H. 2001. Convergent adaptations to cave life in the *Rhamdia laticauda* catfish group
645 (Pimelodidae, Teleostei). Environ. Biol. Fishes 62:251–261.

646 Wilkens, H., and U. Strecker. 2003. Convergent evolution of the cavefish *Astyanax* (Characidae,
647 Teleostei): genetic evidence from reduced eye-size and pigmentation. Biol. J. Linn. Soc. 80:545–
648 554.

649 Williams, S. T. 2012. Advances in molecular systematics of the gastropod superfamily Trochoidea.
650 Zool. Scr. 41:571–595.

651 Williams, S. T., L. M. Smith, D. G. Herbert, B. A. Marshall, A. Warén, S. Kiel, P. Dyal, K. Linse,
652 C. Vilvens, and Y. Kano. 2013. Cenozoic climate change and diversification on the continental
653 shelf and slope: evolution of gastropod diversity in the family Solariellidae (Trochoidea). Ecol.
654 Evol. 3:887–917.

655 Yamamoto, Y., D. W. Stock, and W. R. Jeffery. 2004. Hedgehog signalling controls eye
656 degeneration in blind cavefish. Nature 431:844–7.

657 Zharkova, I. S. 1970. Reduction of the organs of vision in deep sea mysids. Zool. Zhurnal 49:685–
658 693.

659

660 **Table 1 Catalogue data of all specimens examined, with GenBank accession numbers for**
661 **sequence data used in phylogenetic analyses.** Eye morphology data, P, pigmentation present (Y),
662 absent (N), or unknown (?); A, eye aperture open (Y), obscured or closed (N), or unknown (?).
663 Specimens in bold were used in histological studies.

Species	Reg	Locality	Lat/Long	Depth (m)	Expedition/ Station	P	A	28S	COI	16S	12S
Archiminolia 1	MNHN IM-2007-18540	S. Gatukai Island	9°06.9' S, 158° 21' E	267-329	Solomon 2/ DW2301	Y	Y	HF5 861 67	HF5 863 10	HF5 860 19	HF5 858 58
Archiminolia 2	MNHN IM-2007-18316	N Bellona, New Caledonia	20° 23 S, 158° 45’ E	324-330	EBISCO/ CP2572	Y	Y	HF5 861 68	HF5 863 11	HF5 860 20	HF5 858 59
Archiminolia 2	MNHN IM-2007-18339	Norfolk Ridge, Banc Kaimon Maru	23° 24' S, 168° 00' E	400	NORFOLK2 / DW2117	Y	Y	–	–	–	HF5 858 62
Archiminolia 2	MNHN IM-2009-8804	Norfolk Ridge, Banc Antigonia	23° 23' S, 168° 00' E	430-480	TERRASSES/ DW3063	Y	Y	HF5 861 72	HF5 863 15	HF5 860 24	HF5 858 64

Species	Reg	Locality	Lat/Long	Depth (m)	Expedition/ Station	P	A	28S	COI	16S	12S
Archiminolia 2	MNHN IM-2009-8867	Norfolk Ridge, Munida	23° 01' S, 168° 23' E	380-440	TERRASSE S/ DW3107	Y	Y	HF5 86173	HF5 863 16	HF5 860 25	HF5 858 65
Archiminolia 2	MNHN IM-2009-15176	Norfolk Ridge, Munida	23° 01' S, 168° 23' E	380-440	TERRASSE S/ DW3107	Y	Y	–	LT5 75866	–	–
Archiminolia 3	MNHN IM-2013-19973	E Umboi I., Dampier Strait, Papua New Guinea	05°40'S 148°14'E	208-285	PAPUA NIUGUINI/ CP4016	Y	Y	LT5 75948	LT5 7586 7	LT5 7590 5	LT5 7592 4
Archiminolia 3	MNHN IM-2013-19974	E Umboi I., Dampier Strait, Papua New Guinea	05°40'S 148°14'E	208-285	PAPUA NIUGUINI/ CP4016	Y	Y	LT5 75949	LT5 7586 8	LT5 7590 3	LT5 7592 2
Archiminolia 3	MNHN IM-2013-19975	E Umboi I., Dampier Strait, Papua New Guinea	05°40'S 148°14'E	208-285	PAPUA NIUGUINI/ CP4016	Y	Y	LT5 75950	LT5 7586 9	LT5 7590 4	LT5 7592 3

Species	Reg	Locality	Lat/Long	Depth (m)	Expedition/ Station	P	A	28S	COI	16S	12S
Archiminolia oleacea	AM C133269.001	N of Fraser I., Queensland, Australia	24.375°S, 153.285°	192-229	HMAS Kimbla/25	N	?	–	–	–	–
Archiminolia oleacea	AM C133269.001	N of Fraser I., Queensland, Australia	24.375°S, 153.285°	192-229	HMAS Kimbla/25	N	?	–	–	–	–
Archiminolia oleacea	AM C133269.001	N of Fraser I., Queensland, Australia	24.375°S, 153.285°	192-229	HMAS Kimbla/25	N	?	–	–	–	–
Archiminolia oleacea	AM C133269.001	N of Fraser I., Queensland, Australia	24.375°S, 153.285°	192-229	HMAS Kimbla/25	N	?	–	–	–	–

Species	Reg	Locality	Lat/Long	Depth (m)	Expedition/ Station	P	A	28S	COI	16S	12S
Archiminolia oleacea	AM C133269.001	N of Fraser I., Queensland, Australia	24.375°S, 153.285°	192-229	HMAS Kimbla/25	N	?	–	–	–	–
Arxellia helicoides	NHMUK 20140009	Seamount S of Manus I., Papua New Guinea	3°04’S, 147°32’E	402-640	DW3688	Y	Y	HF5 861 57	HF5 863 00	–	HF5 858 46
Arxellia cf. thaumasta	WAM S25779	off Point Hillier, Western Australia	35.3818°S, 117.2030°E	419-460	SS1005/020	Y	Y	–	–	–	–
Arxellia tracheia	MNHN IM-2013-19897	SE Tuam I., Papua New Guinea	06°03'S 148°08'E	440	PAPUA NIUGUINI/ DW4004	Y	Y	–	LT5 9606 7	–	–
Arxellia tracheia	MNHN IM-2013-19898	SE Tuam I., Papua New Guinea	06°03'S 148°08'E	440	PAPUA NIUGUINI/ DW4004	Y	Y	–	LT5 9606 8	–	–

Species	Reg	Locality	Lat/Long	Depth (m)	Expedition/ Station	P	A	28S	COI	16S	12S
Arxellia tracheia	MNHN IM-2013-19899	SE Tuam I., Papua New Guinea	06°03'S 148°08'E	440	PAPUA NIUGUINI/ DW4004	Y	Y	–	LT59606 9	–	–
Arxellia tracheia	MNHN IM-2013-19901	SE Tuam I., Papua New Guinea	06°04'S 148°08'E	440-480	PAPUA NIUGUINI/ DW4005	Y	Y	–	LT59607 0	–	–
Arxellia trochos	MNHN IM-2009-23089	Banc de L'Orne/Walpole, New Caledonia	22°20'S, 169°01'E	400-520	EXBODI/ DW3862	Y	–	LT59606 5	LT59607 2	LT59606 2	LT59605 8
Arxellia trochos	MNHN IM-2009-23092	Banc de L'Orne/Walpole, New Caledonia	22°20'S, 169°01'E	400-520	EXBODI/ DW3862	Y	Y	LT59606 6	LT59607 3	LT59606 3	LT59605 9

Species	Reg	Locality	Lat/Long	Depth (m)	Expedition/ Station	P	A	28S	COI	16S	12S
Arxellia trochos	MNHN IM-2009-23094	Banc de L'Orne/Walpole, New Caledonia	22°19'S, 169°01'E	425-490	EXBODI/ DW3861	–	–	–	LT5 7587 0	–	LT5 7592 5
Arxellia trochos	MNHN IM-2009-23109	Banc Sud Durand, New Caledonia	22°19'S, 168°45'E	471-510	EXBODI/ CP3851	Y	Y	LT5 7595 1	LT5 7587 1	LT5 7590 6	LT5 7592 6
Arxellia trochos	NHMUK 20140006	Banc de L'Orne/Walpole, New Caledonia	22°20'S, 169°01'E	400-520	EXBODI/ DW3862	Y	Y	LT5 9606 4	LT5 9607 1	LT5 9606 1	LT5 9605 7
Bathymophila diadema	MNHN IM-2007-18311	W Bellona, New Caledonia	21° 06' S, 158° 32' E	741-791	EBISCO/ CP2556	Y	N	HF5 860 79	HF5 862 19	HF5 859 29	HF5 857 53
Bathymophila diadema	**MNHN IM-2007-18319**	**SE Fairway, New Caledonia**	**21° 29' S, 162° 36' E**	**883-957**	**EBISCO/ CP2651**	Y	N	**HF5 860 81**	**HF5 862 21**	**HF5 859 31**	**HF5 857 55**

Species	Reg	Locality	Lat/Long	Depth (m)	Expedition/ Station	P	A	28S	COI	16S	12S
Bathymophila diadema	MNHN IM-2007-18320	SE Fairway, New Caledonia	21° 29' S, 162° 36' E	883-957	EBISCO/ CP2651	Y	N	HF5 860 82	HF5 862 22	HF5 859 32	HF5 857 56
Bathymophila diadema	MNHN IM-2007-18535	NW Vella, Lavella I., Solomon Islands	7° 31.3' S, 156° 17.7' E	782-884	SALOMON 2/ CP2249	Y	N	–	HF5 862 23	–	HF5 857 25
Bathymophila diadema	MNHN IM-2009-8869	Loyalty Ridge	23° 48' S, 169° 46' E	660-710	TERRASSE S/ DW3045	Y	N	HF5 860 84	HF5 862 26	HF5 859 34	HF5 857 61
Bathymophila diadema	MNHN IM-2009-8871	Loyalty Ridge	23° 48' S, 169° 46' E	660-710	TERRASSE S/ DW3045	Y	N	HF5 860 85	HF5 862 27	HF5 859 35	HF5 857 62

Species	Reg	Locality	Lat/Long	Depth (m)	Expedition/ Station	P	A	28S	COI	16S	12S
Bathymophila diadema	MNHN IM-2009-13010	NW Vella, Lavella I., Solomon Islands	7° 31.3' S, 156° 17.7' E	782-884	SALOMON 2/ CP2249	Y	N	–	–	–	HF5857 57
Bathymophila diadema	MNHN IM-2009-13011	NW Vella, Lavella I., Solomon Islands	7° 31.3' S, 156° 17.7' E	782-884	SALOMON 2/ CP2249	Y	N	–	HF5862 24	–	HF5857 58
Bathymophila diadema	MNHN IM-2009-13012	NW Vella, Lavella I., Solomon Islands	7° 31.3' S, 156° 17.7' E	782-885	SALOMON 2/ CP2249	Y	N	–	–	–	–
Bathymophila diadema	MNHN IM-2009-15191	Off Bougainville, Papua New Guinea	5° 04' S, 154° 29' E	662	BIOPAPUA/ CP3755	Y	N	HF5860 88	HF5862 29	HF5859 38	HF5857 64
Bathymophila diadema	MNHN IM-2009-15198	Off Bougainville, Papua New Guinea	05°02’S, 154°29’E	615-632	BIOPAPUA/ DW3754	Y	N	–	LT57587 2	–	–

Species	Reg	Locality	Lat/Long	Depth (m)	Expedition/ Station	P	A	28S	COI	16S	12S
Bathymophila diadema	MNHN IM-2009-15199	Off Bougainville, Papua New Guinea	05°02’S, 154°29’E	615-632	BIOPAPUA/ DW3754	Y	N	–	LT57587 3	–	–
Bathymophila diadema	MNHN IM-2009-15200	Off Bougainville, Papua New Guinea	05°02’S, 154°29’E	615-632	BIOPAPUA/ DW3754	Y	N	–	LT57587 4	–	–
Bathymophila diadema	MNHN IM-2009-15217	Off Bougainville, Papua New Guinea	05°04’S, 154°29’E	662	BIOPAPUA/ CP3755	Y	N	–	–	–	LT59606 0
Bathymophila diadema	MNHN IM-2009-15221	Off Bougainville, Papua New Guinea	05°04’S, 154°29’E	662	BIOPAPUA/ CP3755	Y	N	–	–	–	–
Bathymophila sp 2	MNHN IM-2007-18323	Chesterfield, New Caledonia	19° 38' S, 158° 44' E	569-570	EBISCO/ DW2584	Y	N	HE800722	HE800623	HE800762	HE800673

Species	Reg	Locality	Lat/Long	Depth (m)	Expedition/ Station	P	A	28S	COI	16S	12S
Bathymophila sp 4	MNHN IM-2009-8762	Between Nosy-bé and Banc du Leven, Madagascar	12° 47' S, 48° 08' E	784	MIRIKY/ CP3221	Y	N	HF5 860 89	HF5 862 30	HF5 859 39	HF5 857 65
Bathymophila sp 4	MNHN IM-2009-8764	Between Nosy-bé and Banc du Leven, Madagascar	12° 47' S, 48° 08' E	783	MIRIKY/ CP3221	Y	N	HF5 860 91	HF5 862 32	–	HF5 857 67
Bathymophila sp 4	MNHN IM-2009-8769	Between Nosy-bé and Banc du Leven, Madagascar	12° 26' S, 48° 13'E,	578-782	MIRIKY/ CP3192	Y	N	HF5 860 92	HF5 862 33	HF5 859 41	HF5 857 68
Bathymophila sp 4	MNHN IM-2009-8770	Between Nosy-bé and Banc du Leven, Madagascar	12° 34' S, 48° 09' E	613-625	MIRIKY/ CP3186	Y	N	HF5 860 93	HF5 862 34	HF5 859 42	HF5 857 69

Species	Reg	Locality	Lat/Long	Depth (m)	Expedition/ Station	P	A	28S	COI	16S	12S
Bathymophila sp 4	MNHN IM-2009-8772	Between Nosy-bé and Banc du Leven, Madagascar	12° 47' S, 48° 08' E	782	MIRIKY/ CP3221	Y	N	HF5 860 95	HF5 862 36	HF5 859 44	HF5 857 71
Bathymophila sp 4	MNHN IM-2009-8773	Between Nosy-bé and Banc du Leven, Madagascar	12° 47' S, 48° 08' E	782	MIRIKY/ CP3221	Y	N	HF5 860 96	HF5 862 37	HF5 859 45	HF5 857 72
Bathymophila sp 7	MNHN IM-2007-18317	SE Fairway, New Caledonia	21° 29' S, 162° 36'E	883-957	EBISCO/ CP2651	N	?	HF5 860 98	HF5 862 39	HF5 859 47	HF5 857 74
Bathymophila n.s. 7	MNHN IM-2009-23095	Ile Matthew-Volcan, New Caledonia	22°19'S, 171°20'E	925	EXBODI/ DW3879	N	?	LT5 7595 2	LT5 7587 6	LT5 7590 7	LT5 7592 7

Species	**Reg**	**Locality**	**Lat/Long**	**Depth (m)**	**Expedition/ Station**	**P**	**A**	**28S**	**COI**	**16S**	**12S**
Bathymophila sp 9	MNHN IM-2007-35590	Grand Passage, New Caledonia	19° 00' S, 163° 26' E	285-300	CONCALIS/ DW3023	N	?	HF5 86100	HF5 862 41	HF5 859 49	HF5 857 79
Bathymophila sp 10	MNHN IM-2009-15182	Vitiaz Straight, Papua New Guinea	05° 59' S, 147° 39'E	860-880	BIOPAPUA/ CP3724?	N	?	HF5 86101	HF5 862 42	HF5 859 50	HF5 857 81
Bathymophila sp 11	MNHN IM-2009-15175	Niau, Tuamotu Archipelago	16° 08' S, 146° 24'W	412-520	TARASOL/ DW3369	N	?	HF5 86102	HF5 862 43	HF5 859 51	HF5 857 87
***Bathymophila n.s.* 18**	**MNHN IM-2009-23080**	**Ile Matthew-Volcan, New Caledonia**	**22°19'S, 171°20'E**	**925**	**EXBODI/ DW3879**	**N**	**Y**	LT5 75953	LT5 7587	LT5 7590	LT5 7592

Species	Reg	Locality	Lat/Long	Depth (m)	Expedition/ Station	P	A	28S	COI	16S	12S
Bathymophila n.s. 18	MNHN IM-2009-23100	Ile Matthew-Volcan, New Caledonia	22°19'S, 171°20'E	925	EXBODI/ DW3879	N	?	LT5 7595 4	LT5 7588 0	LT5 7590 9	LT5 7593 0
Bathymophila n.s. 18	MNHN IM-2009-23101	Ile Matthew-Volcan, New Caledonia	22°19'S, 171°20'E	925	EXBODI/ DW3879	N	?	LT5 7595 5	LT5 7587 9	LT5 7591 2	LT5 7593 1
Bathymophila n.s. 18	MNHN IM-2009-23103	Ile Matthew-Volcan, New Caledonia	22°19'S, 171°20'E	925	EXBODI/ DW3879	N	?	LT5 7595 7	–	LT5 7591 0	LT5 7592 8
Bathymophila n.s. 18	MNHN IM-2009-23104	Ile Matthew-Volcan, New Caledonia	22°19'S, 171°20'E	925	EXBODI/ DW3879	N	?	LT5 7595 6	LT5 7587 8	LT5 7591 1	LT5 7593 2

Species	Reg	Locality	Lat/Long	Depth (m)	Expedition/ Station	P	A	28S	COI	16S	12S
Bathymophila n.s. 19	MNHN IM-2009-23081	N Ile Matthew-Volcan, New Caledonia	22°17'S, 171°18'E	785	EXBODI/ DW3877	N	?	LT5 7596 0	–	LT5 7591 4	LT5 7593 5
Bathymophila n.s. 20	MNHN IM-2009-23082	Ile Matthew-Volcan, New Caledonia	22°19'S, 171°20'E	925	EXBODI/ DW3879	N	?	LT5 7595 8	LT5 7588 1	–	LT5 7593 3
Bathymophila n.s. 20	MNHN IM-2009-23102	Ile Matthew-Volcan, New Caledonia	22°19'S, 171°20'E	925	EXBODI/ DW3879	N	?	LT5 7595 9	LT5 7588 2	LT5 7591 3	LT5 7593 4
Bathymophila sp 21	MNHN IM-2009-15206	Seamounts near Bougainville, Papua New Guinea	05°33’S, 153°59’E	458	BIOPAPUA/ CP3747	Y	Y	–	LT5 7587 5	–	–

Species	Reg	Locality	Lat/Long	Depth (m)	Expedition/ Station	P	A	28S	COI	16S	12S
Clade B sp 2	MNHN IM-2009-8739	Mozambique Channel	23° 33' S, 36° 02' E	886-898	MAINBAZ A/ CP3140	Y	Y	HE800720	HE800621	HE800760	HE800671
Clade B sp 2	MNHN IM-2009-8742	Maputo transect, Mozambique Channel	23° 33' S, 36° 02' E	886-898	MAINBAZ A/ CP3140	Y	Y	HF586070	HF586211	HF585920	HF585744
Elaphriella khantaros	MNHN IM-2009-15201	Near Bougainville, Papua New Guinea	05°04’S, 154°29’E	662	BIOPAPUA/ CP3755	Y	N	–	LT757883	–	–
Elaphriella khantaros	MNHN IM-2009-15214	Off Bougainville, Papua New Guinea	05°02’S, 154°29’E	615-632	BIOPAPUA/ CP3754	Y	N	–	–	–	LT757936
Elaphriella khantaros	MNHN IM-2009-15218	Off Bougainville, Papua New Guinea	05°04’S, 154°29’E	662	BIOPAPUA/ CP3755	Y	N	–	–	–	–

Species	Reg	Locality	Lat/Long	Depth (m)	Expedition/ Station	P	A	28S	COI	16S	12S
Elaphriella khantaros	MNHN IM-2009-15220	W of New Hanover, Papua New Guinea	02°13’S, 150°23’E	680-700	BIOPAPUA/ CP3653	Y	N	–	–	–	LT5 7593 7
Elaphriella khantaros	MNHN IM-2009-15235	W of New Hanover, Papua New Guinea	02°13’S, 150°23’E	680-700	BIOPAPUA/ CP3653	Y	N	–	–	–	–
Elaphriella khantaros	MNHN IM-2009-15236	W of New Hanover, Papua New Guinea	02°13’S, 150°23’E	680-700	BIOPAPUA/ CP3653	Y	N	–	–	–	–
Elaphriella khantaros	MNHN IM-2009-33821	Off Bougainville, Papua New Guinea	05°02’S, 154°29’E	615-632	BIOPAPUA/ DW3754	Y	N	–	–	–	–
Elaphriella khantaros	**MNHN IM-2009-43073**	**W. Vella, Solomon Islands**	**7° 42.9' S, 156° 27.3' E**	**518-527**	**SALOMON 2/CP2243**	**Y**	**N**	**HF5 860 63**	**HF5 862 08**	**HF5 859 13**	**HF5 857 36**

Species	**Reg**	**Locality**	**Lat/Long**	**Depth (m)**	**Expedition/ Station**	**P**	**A**	**28S**	**COI**	**16S**	**12S**
Elaphriella new species	MNHN IM-2013-19896	SE Tuam I., Papua New Guinea	06°03'S 148°08'E	440	PAPUA NIUGUINI/ DW4004	Y	Y	LT5 7596 1	LT5 7588 4	LT5 7591 5	LT5 7593 8
Elaphriella paulinae	MNHN IM-2009-23099	Banc Sud Durand, New Caledonia	22°18'S, 168°46'E	692	EXBODI/ CP3853	Y	N	–	LT5 7588 5	–	–
Elaphriella wareni	**MNHN IM-2009-18318**	**SE Fairway, New Caledonia**	**21°29'S, 162°36'E**	**883-957**	**EBISCO/ CP2651**	**N**	**N**	**HF5 860 58**	**–**	**HF5 859 08**	**HF5 857 29**
Ilanga 1	MNHN IM-2009-15207	Seamounts near Bougainville, Papua New Guinea	05°37'S, 154°01'E	398-399	BIOPAPUA/ DW3748	Y	Y	–	LT5 7588 6	–	–
Ilanga 1	MNHN IM-2009-15208	Seamounts near Bougainville, Papua New Guinea	05°37'S, 154°01'E	398-399	BIOPAPUA/ DW3748	Y	Y	–	LT5 7588 8	–	–

Species	**Reg**	**Locality**	**Lat/Long**	**Depth (m)**	**Expedition/ Station**	**P**	**A**	**28S**	**COI**	**16S**	**12S**
Ilanga 1	MNHN IM-2009-15209	Seamounts near Bougainville, Papua New Guinea	05°37’S, 154°01’E	398-399	BIOPAPUA/ DW3748	Y	Y	–	LT5 7588 7	–	–
Ilanga 1	MNHN IM-2009-15237	Seamounts near Bougainville, Papua New Guinea	05°37’S, 154°01’E	398-399	BIOPAPUA/ DW3748	Y	Y	–	LT5 7588 9	–	–
***Ilanga* 6**	**MNHN IM-2009-31831**	**E Aoré Island, off Aimbuei Bay, Vanuatu**	**15°34.9'S, 167°13.9’E**	**10-51**	**SANTO2006/EP35**	Y	Y	**–**	LT5 7589 0	**–**	**–**
Ilanga 10	MNHN IM-2009-8797	SE Terrasses, New Caledonia	22° 13' S, 167° 12' E	360-380	TERRASSES/ CP3092	Y	Y	–	–	–	HF5 858 28
Ilanga 10	MNHN IM-2009-15222	SE Terrasses, New Caledonia	22.19°S, 167.16°E	360-380	TERRASSES/ CP3092	Y	Y	–	LT5 7589 1	–	–

Species	**Reg**	**Locality**	**Lat/Long**	**Depth (m)**	**Expedition/ Station**	**P**	**A**	**28S**	**COI**	**16S**	**12S**
Ilanga 10	MNHN IM-2009-15223	SE Terrasses, New Caledonia	22.19°S, 167.16°E	360-380	TERRASSES/ CP3092	Y	Y	–	LT575892	–	–
Ilanga 10	MNHN IM-2009-15224	SE Terrasses, New Caledonia	22.19°S, 167.16°E	360-380	TERRASSES/ CP3092	Y	Y	–	LT575893	–	–
Ilanga 10	MNHN IM-2009-15225	SE Terrasses, New Caledonia	22.19°S, 167.16°E	360-380	TERRASSES/ CP3092	Y	Y	–	LT575894	–	–
Ilanga 10	MNHN IM-2009-15226	SE Terrasses, New Caledonia	22.19°S, 167.16°E	360-380	TERRASSES/ CP3092	Y	Y	–	LT575895	–	–
***Ilanga* 10**	**MNHN IM-2009-23091**	**Off Yaté, New Caledonia**	**22°06'S, 167°06'E**	**325-346**	**EXBODI/ CP3833**	Y	Y	**–**	LT575896	**–**	LT575939

Species	Reg	Locality	Lat/Long	Depth (m)	Expedition/ Station	P	A	28S	COI	16S	12S
Ilanga 10	MNHN IM-2009-23098	Off Yaté, New Caledonia	22°02'S 167°04'E	325-332	EXBODI/ CP3833	Y	Y	–	–	–	LT5 7594 0
Ilanga 10	MNHN IM-2009-43071	Canal de la Havannah, New Caledonia	22°14'S, 167°11'E	378-414	EXBODI/ CP3790	Y	Y	–	–	–	LT5 7594 0
Ilanga n.s. 21	WAM S84074	Off Red Bluff, Western Australia	24° 1.03'S, 113° 2.03'E	100-101	Southern Surveyor/ SS1005/133	Y	Y	LT5 7596 2	LT5 7589 7	LT5 7591 6	LT5 7594 2
Microgaza rotella	MNHN IM-2013-8023	Guadeloupe	16° 24'N, 61° 33'W	130	KARUBEN THOS 2012/GD33	Y	Y	LT5 7596 4	LT5 7590 2	LT5 7592 0	LT5 7594 7
Microgaza rotella	MNHN IM-2013-8051	Guadeloupe	16° 24.97'N, 61° 33.8'W	85	KARUBEN THOS 2012/GD31	Y	Y	LT5 7596 5	LT5 7589 8	LT5 7591 8	LT5 7594 6

Species	Reg	Locality	Lat/Long	Depth (m)	Expedition/ Station	P	A	28S	COI	16S	12S
Microgaza rotella	MNHN IM-2013-9016	Nord Pointe des Chateaux, Guadeloupe	16° 16.42'N, 61° 10.22'W	100	KARUBEN THOS 2012/GD70	Y	Y	LT5 75966	LT5 75900	LT5 75921	LT5 75945
Microgaza rotella	MNHN IM-2013-20336	Le Moule, Guadeloupe	16° 19.9'N, 61° 19.47'W	1	KARUBEN THOS 2012/GM14	Y	Y	LT5 75963	LT5 75899	LT5 75917	LT5 75943
Microgaza rotella	MNHN IM-2013-31167	Guadeloupe	16° 25'N, 61° 33'W	120	KARUBEN THOS 2012/GN22	Y	Y	LT5 75967	LT5 75901	LT5 75919	LT5 75944
Solariella 6	MNHN IM-2007-18537	Russel Island, W.Bay, Solomon Is	9° 1.1' S, 159° 05.7' E	100-200	SALOMON 2/DW2169	Y	Y	–	HF5 86338	–	HF5 85891

Species	Reg	Locality	Lat/Long	Depth (m)	Expedition/ Station	P	A	28S	COI	16S	12S
Solariella obscura	SMNH-106159	Matochkin Strait, Russia	73°30'N, 57°50'E	9	Jenissej 1875/76	Y	Y	–	–	–	–
Solariella obscura	SMNH-106161	W of Novaya Zemlya, Arctic Ocean	79°37'N, 52°30'E	36	Jenissej 1875/52	Y	Y	–	–	–	–
'Solariella' varicosa	NHMUK 20120235	Finnmark county, Varangerfjorden, SW of Vestre Jakobselv, Norway	70° 4.00' N, 29° 12.00' E	10-174	R/V 'Asterias'	Y	Y	–	–	–	HF5857020
Solariella varicosa	SMNH-106152	Mossel Bay, W Spitsbergen, Svalbard	79°50'N, 15°30'E	13-16	Swedish Polar/143	Y	Y	–	–	–	–
Solariella varicosa	SMNH-106154	Matochkin Strait, Russia	73°30'N, 57°50'E	43-44	Jenissej 1875/72	N	?	–	–	–	–

Species	**Reg**	**Locality**	**Lat/Long**	**Depth (m)**	**Expedition/ Station**	**P**	**A**	**28S**	**COI**	**16S**	**12S**
Solariella varicosa	SMNH-106155	Mossel Bay, W Spitsbergen	79°60'N, 15°20'E	22	Swedish Polar/132	Y	Y	–	–	–	–
Spectamen 1	MNHN IM-2007-18351	W Pamilacan Island, Philippines	9°30'N, 123° 50'E	100-138	PANGLAO2 004/T39	Y	Y	HF5 861 86	HF5 863 31	HF5 860 38	HF5 858 81
Spectamen laevior	MNHN IM-2007-18428	Bohol Sea, Philippines	9°28.4’N, 123°50’E	128-142	PANGLAO2 005/CP2344	Y	Y	HF5 861 87	HF5 863 32	HF5 860 39	HF5 858 82
Spectamen mutabilis	**MNHN IM-2009-28738**	**Philippines**	**14° 46' N, 123° 40' E**	**357-367**	**AURORA/ CP2695**	Y	Y	**HF5 861 88**	**HF5 863 34**	**–**	**HF5 858 84**
Zetela 1	MNHN IM-2009-15167	Mozambique Channel	25°13’S, 35°21’E	700-707	MAINBAZ A/ CP3138	Y	?	HF5 861 94	HF5 863 39	HF5 860 45	HF5 857 86

Species	**Reg**	**Locality**	**Lat/Long**	**Depth (m)**	**Expedition/ Station**	**P**	**A**	**28S**	**COI**	**16S**	**12S**
Zetela 1	MNHN IM-2009-15169	Mozambique Channel	25°13’S, 35°21’E	700-707	MAINBAZ A/ CP3138	Y	?	–	HF5 863 40	HF5 860 46	HF5 858 93
***Zetela* 1**	**MNHN IM-2009-8748**	**Mozambique Channel**	**25° 13' S, 35° 21' E**	**700-707**	**MAINBAZ A/ CP3138**	**Y**	**?**	**HF5 861 95**	**HF5 863 41**	**HF5 860 47**	**HF5 858 95**
Zetela 2	NHMUK 20120236	Eastern Weddell Sea, Antarctica	71° 18.35' S, 13° 57.71' W	1030	ANDEEP III/ PS67/074-6-E	Y	Y	HF5 860 50	HF5 861 99	HF5 858 98	HF5 857 14
Zetela 2	BAS KL05-0328	Antarctica	71° 18.35' S 13° 57.71' W	1030	ANDEEP III/ PS67/074-6-E	Y	Y	–	–	–	–

Species	**Reg**	**Locality**	**Lat/Long**	**Depth (m)**	**Expedition/ Station**	**P**	**A**	**28S**	**COI**	**16S**	**12S**
Zetela 3	NHMUK 20120240	Burdwood Bank, Antarctica	54° 30.22' S, 56° 8.20' W	286-290	LAMPOS ANDEEP/15 0-1	Y	Y	HF5 860 54	HF5 862 04	HF5 859 03	HF5 857 19
Zetela alphonsi	ZSM 20041246	Región del BioBío, Chile	36°24.1'S, 73°36.4'W	600	–	N	?	–	–	–	–
Zetela alphonsi	ZSM 20041458	Región del BioBío, Chile	36°24.1'S, 73°36.4'W	600	–	N	?	–	–	–	–
Zetela alphonsi	**ZSM-MOL-20041247**	**Región del BioBío, Chile**	**36°24.1'S, 73°36.4'W**	**600**	**–**	N	**N**	**–**	**–**	**–**	**–**

664

Figure 1 A typical solariellid eye (sagittal plane). The eye consists of an invaginated epithelial cup, which remains narrowly open, allowing light to enter. Rhabdomeric photoreceptors are surrounded by apically pigmented retinal cells and a central vitreous body acts as a lens.

Figure 2 Eye morphology in solariellid species studied histologically. Variety in eye morphology is evident in different species even from external examination, as shown here. **A**, *Ilanga* 10 (typical eye); **B**, *Bathymophila diadema* (with eye covered by skin); **C**, *Elaphriella wareni* (lacking pigment)*;* **D** '*Bathymophila'* 18 (lacking pigment). **E**, *Spectamen mutabilis* (typical eye); **F**, *Zetela* 1 (half pigmented, atypical shape); **G**, *Ilanga* 6 (typical eye); **H**, *Elaphriella khantaros* (with eye covered by skin); CT, cephalic tentacle; es, eyestalk; ey, eye. Scale bars, 500 µm.

Figure 3 Variety in solariellid eye anatomy. Semi-thin sections, taken through the eye along a sagittal plane as in Figure 1, and tomographic modelling demonstrate the full extent of variety of eye structures and deviations from the typical eye (Figure 1) in different species. Left, photograph with superimposed tomographic model of eye structure; right, section through the eye. Four species as in Figure 2; also compare phylogenetic positions in Figure 4. **A**, *Ilanga* 10; **B**, *Bathymophila diadema*; **C**, *Elaphriella wareni;* **D** '*Bathymophila'* 18. Ap, eye aperture; epi, epithelium; mv, microvillous layer; ner, optic nerve; pr, photoreceptors; ret, retina. Scale bars, 50 µm.

Figure 4 Time-calibrated solariellid phylogeny mapping eye morphs, species depth range and proposed occurrence of eye reduction events in all examined species. Branch lengths are proportional to time (scale below in millions of years) based on the BEAST reconstruction. Node support values are posterior probabilities. Light horizontal bars on nodes correspond to 95% highest posterior density (HPD) interval for node ages (i.e. the shortest interval that contains 95%

688 of the sampled values). Three time calibrations are indicated: 1, ingroup calibration; 2, *Solariella*
689 calibration, 3, *Zetela* calibration; see Williams et al. (2013) for further details. Species in bold were
690 studied histologically and a schematic diagram of eye anatomy is shown. Remaining species were
691 examined externally. Two species noted with dotted lines, *Archiminolia oleacea* and *Zetela*
692 *alphonsi*, were not included in molecular analyses and occupy unresolved positions in their
693 accepted genera. Events are plotted at the earliest point where the reduced state is the most
694 parsimonious or where proportional likelihood at the succeeding node is greater than 0.95 for the
695 reduced state. Tree topology follows the BEAST tree, with a single specimen representing each
696 species. Vertical grey bars represent important geological events: Cretaceous-Tertiary boundary
697 (66 Ma), Palaeocene-Eocene thermal maximum (55.5 Ma) and Eocene-Oligocene transition (34
698 Ma).

699

700

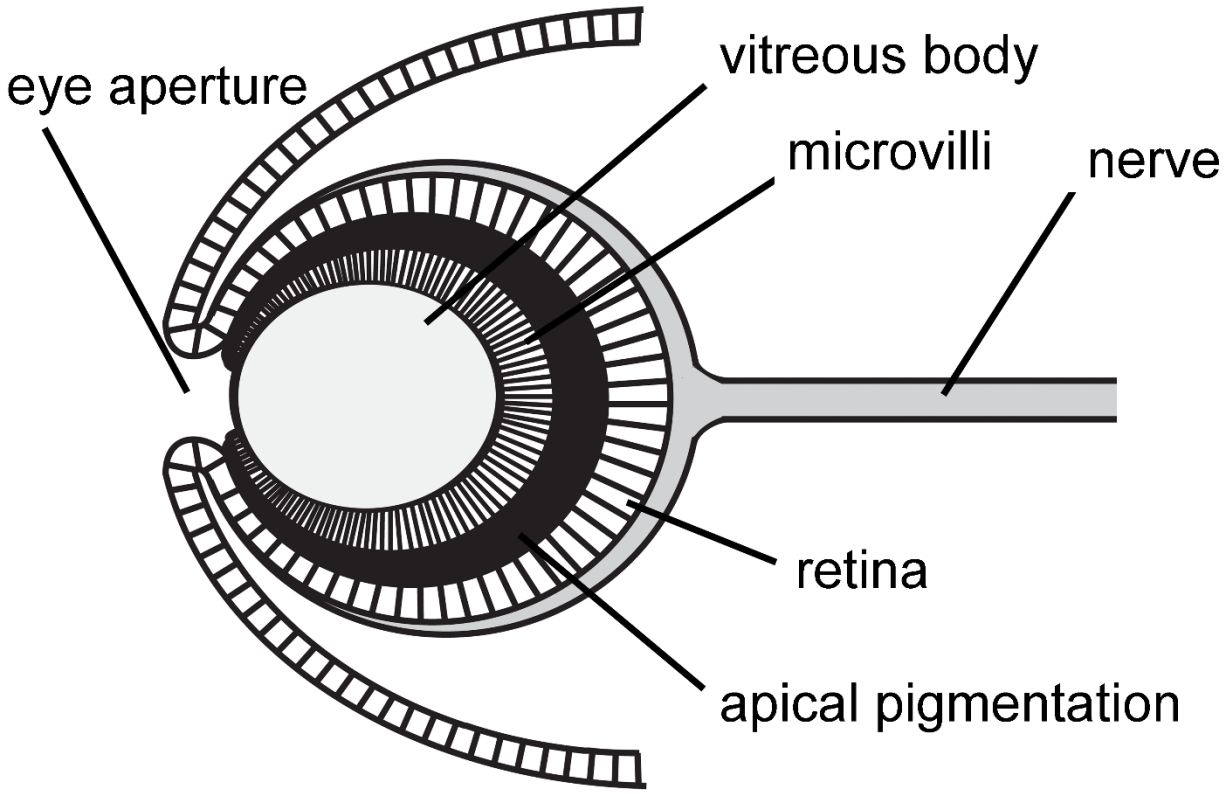
eye aperture
vitreous body
microvilli
nerve
retina
apical pigmentation

701

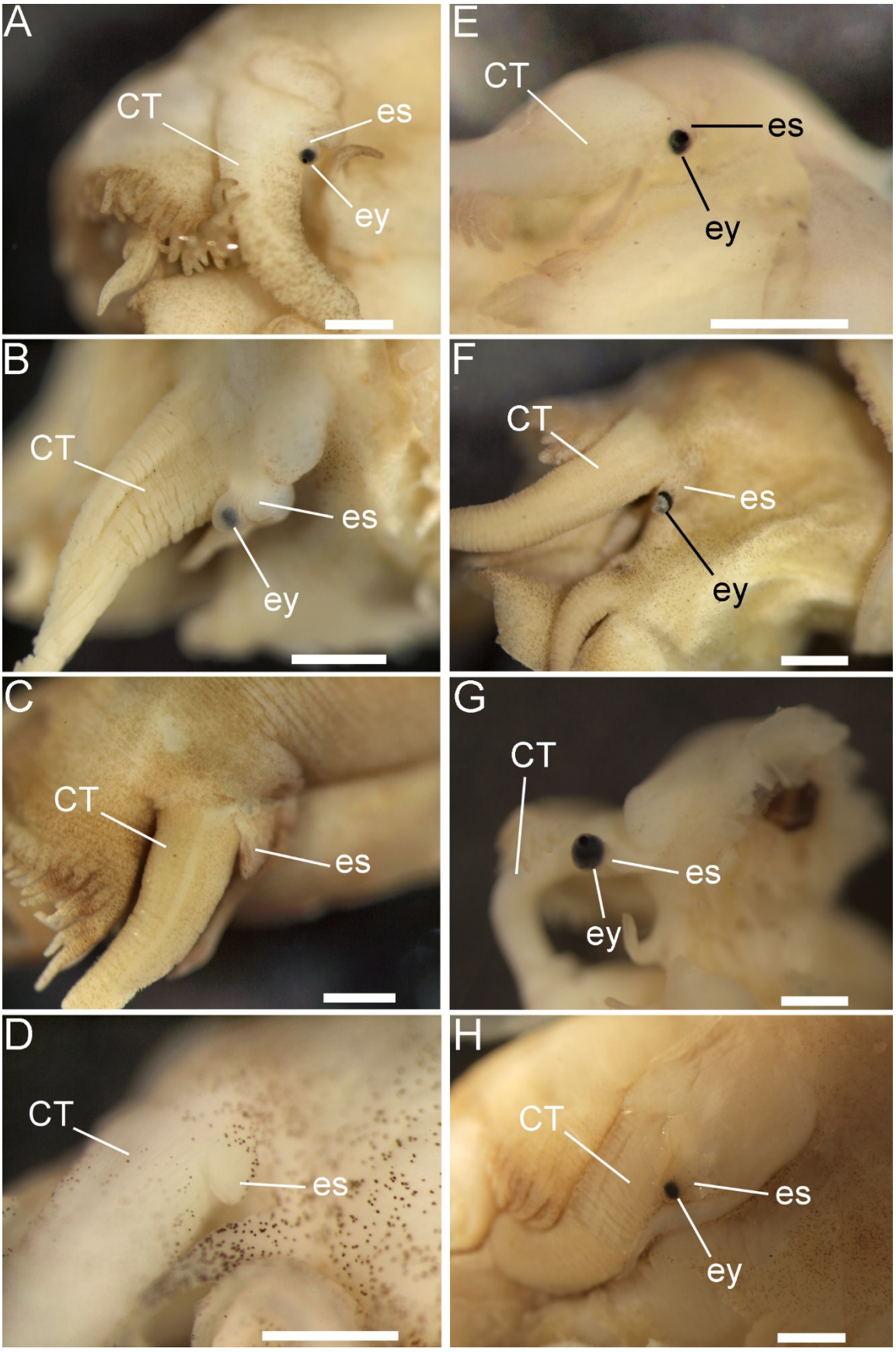
A
CT
es
ey
E
CT
es
ey
B
CT
es
ey
F
CT
es
ey
C
CT
es
G
CT
es
ey
D
CT
es
H
CT
es
ey

702

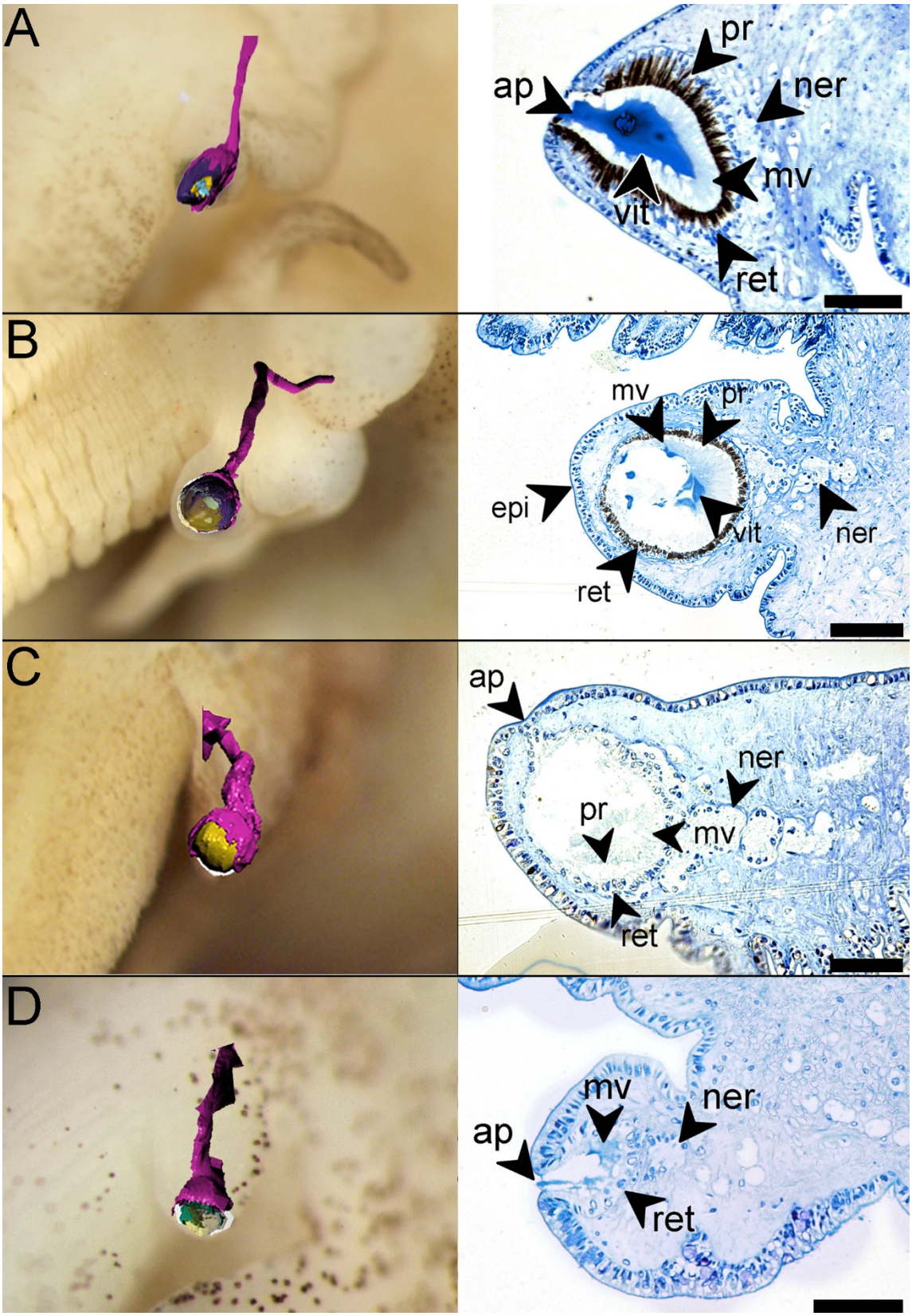
A
pr
ap
ner
mv
vit
ret
B
mv
pr
epi
vit
ner
ret
C
ap
ner
pr
mv
ret
D
mv
ner
ap
ret

703

704

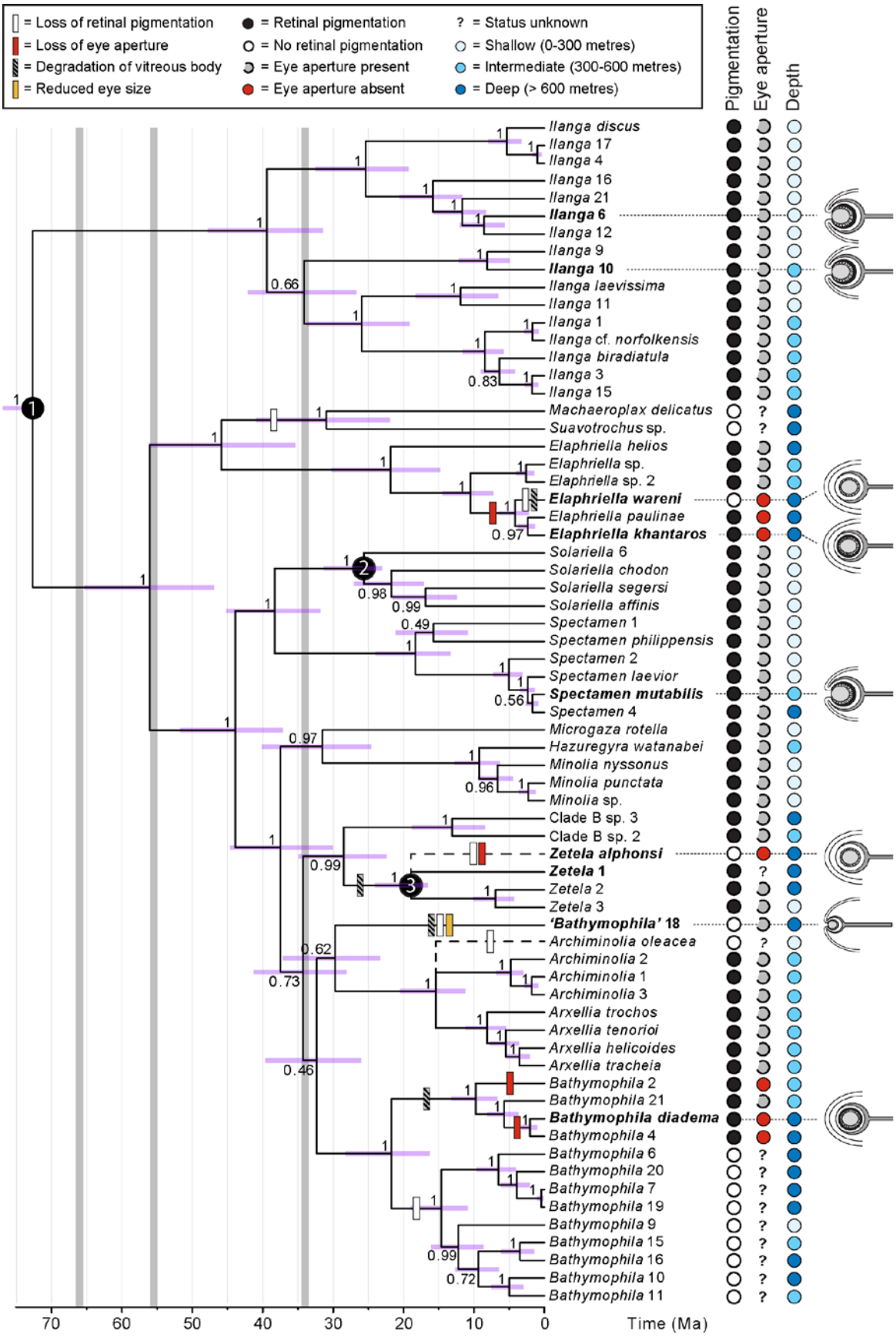
= Loss of retinal pigmentation
= Loss of eye aperture
= Degradation of vitreous body
= Reduced eye size
= Retinal pigmentation
= No retinal pigmentation
= Eye aperture present
= Eye aperture absent
? = Status unknown
= Shallow (0-300 metres)
= Intermediate (300-600 metres)
= Deep (> 600 metres)
Pigmentation
Eye aperture
Depth
Ilanga discus
Ilanga 17
Ilanga 4
Ilanga 16
Ilanga 21
Ilanga 6
Ilanga 12
Ilanga 9
Ilanga 10
Ilanga laevissima
Ilanga 11
Ilanga 1
Ilanga cf. norfolkensis
Ilanga biradiatula
Ilanga 3
Ilanga 15
Machaeroplax delicatus
Suavotrochus sp.
Elaphriella helios
Elaphriella sp.
Elaphriella sp. 2
Elaphriella wareni
Elaphriella paulinae
Elaphriella khantaros
Solariella 6
Solariella chodon
Solariella segersi
Solariella affinis
Spectamen 1
Spectamen philippensis
Spectamen 2
Spectamen laevior
Spectamen mutabilis
Spectamen 4
Microgaza rotella
Hazuregyra watanabei
Minolia nyssonus
Minolia punctata
Minolia sp.
Clade B sp. 3
Clade B sp. 2
Zetela alphonsi
Zetela 1
Zetela 2
Zetela 3
'Bathymophila' 18
Archiminolia oleacea
Archiminolia 2
Archiminolia 1
Archiminolia 3
Arxellia trochos
Arxellia tenorioi
Arxellia helicoides
Arxellia tracheia
Bathymophila 2
Bathymophila 21
Bathymophila diadema
Bathymophila 4
Bathymophila 6
Bathymophila 20
Bathymophila 7
Bathymophila 19
Bathymophila 9
Bathymophila 15
Bathymophila 16
Bathymophila 10
Bathymophila 11
70
60
50
40
30
20
10
0
Time (Ma)

705

Supplementary Data files

Supplementary Data 1 as PDF: Phylogenetic reconstruction using combined MrBayes analysis of COI, 12S, 18S and 28S fragments for all available specimens (n = 119). Nodes with less than 50% support have been collapsed.

Supplementary Data 2 as PDF: Phylogenetic reconstruction using MrBayes for COI fragments for all available specimens (n = 201). Nodes with less than 50% support have been collapsed.

Supplementary Data 3 as PDF: Phylogenetic reconstruction using MrBayes for 12S fragments for all available specimens (n = 225). Nodes with less than 50% support have been collapsed.

Supplementary Data 4 as PDF: Ancestral state reconstructions for four morphological characters of the eye. Topology and branch lengths based on results from time-calibrated BEAST analysis (Figure 4). Scale bar below in millions of years. Black indicates ancestral state (intact eye), red indicates a reduced feature. Grey colouring indicates character state unknown (proportional likelihoods of neither character state significant at the 0.05 level). **A**, status of retinal pigmentation reconstructed (black, normally pigmented; red, pigmentation absent); **B**, status of the eye aperture (black, open; red, obscured); **C**, eye size (black, normal; red, reduced); **D**, nature of the vitreous body (black, intact; red, degraded). Note that the incidence or absence of pigmentation does not appear to correlate well with any of the other three characters indicated.

*Supplementary Data 5 as PDF***:** Tomographic models of eye anatomy in Solariellidae. Click image to activate, then click and drag to manipulate or select previews and tissue types from the drop-down menu.

Supplementary Data 6 as PDF: Collection and sequence data for all specimens included in phylogenetic analyses, including those not examined for eye morphology.